


$P_{\psi s}^{\Lambda}(4338)$ pentaquark and its partners in the molecular pictureMao-Jun Yan¹, Fang-Zheng Peng,² Mario Sánchez Sánchez,³ and Manuel Pavon Valderrama^{2,*}¹CAS Key Laboratory of Theoretical Physics, Institute of Theoretical Physics,
Chinese Academy of Sciences, Beijing 100190, China²School of Physics, Beihang University, Beijing 100191, China³LP2IB (CNRS/IN2P3—Université de Bordeaux), 33175 Gradignan cedex, France (Received 8 September 2022; accepted 18 March 2023; published 19 April 2023)

The LHCb collaboration has detected a new hidden-charm pentaquark with the quantum numbers of a Λ baryon: the $P_{\psi s}^{\Lambda}(4338)$. This pentaquark will be interpreted as a $\bar{D}_s\Lambda_c - \bar{D}\Xi_c$ resonance within a contact-range theory. Here we briefly comment on the relation of the new $P_{\psi s}^{\Lambda}(4338)$ with the $P_{\psi s}^{\Lambda}(4459)$. We find that the $P_{\psi s}^{\Lambda}(4338)$ and $P_{\psi s}^{\Lambda}(4459)$ both accept a common description in terms of the same parameters, which predicts the existence of a few additional $P_{\psi s}^N$, $P_{\psi s}^{\Lambda}$, $P_{\psi s}^{\Sigma}$, and $P_{\psi ss}^{\Xi}$ molecular pentaquarks composed of a charmed antimeson and an antitriplet charmed baryon. The most robust of these predicted pentaquarks is a $P_{\psi s}^{\Lambda}$ with a mass in the (4235–4255) MeV range, while other two interesting ones are a $P_{\psi s}^N(4150)$ and a $P_{\psi s}^{\Sigma}(4335)$, the latter basically at the same mass as the $P_{\psi s}^{\Lambda}(4338)$, with which it might mix owing to isospin symmetry breaking effects.

DOI: [10.1103/PhysRevD.107.074025](https://doi.org/10.1103/PhysRevD.107.074025)**I. INTRODUCTION**

Recently the LHCb collaboration has announced [1,2] the discovery of a new pentaquark with mass and width

$$\begin{aligned} M &= 4338.2 \pm 0.7 \text{ MeV}, \\ \Gamma &= 7.0 \pm 1.2 \text{ MeV}, \end{aligned} \quad (1)$$

which has been observed in the $J/\psi\Lambda$ mass distribution of the $B^- \rightarrow J/\psi\Lambda\bar{p}$ decay. It has been named the $P_{\psi s}^{\Lambda}(4338)$ [in the new convention from [3], or $P_{cs}(4338)$ in the previous, widely used convention], has the light-quark content of a Λ baryon, and its spin-parity is $J^P = \frac{1}{2}^-$. In addition, there seems to be hints of a nontrivial structure in the $J/\psi\bar{p}$ mass distribution, maybe pointing out towards a possible $P_{\psi s}^N$ hidden-charm pentaquark (where the superscript indicates that its light-quark content is that of the nucleon).

Here we explore the nature of the new $P_{\psi s}^{\Lambda}(4338)$ pentaquark. Within the molecular picture it fits well as a heavy-quark spin symmetry (HQSS) partner of the $P_{\psi s}^{\Lambda}(4459)$ [4] (often interpreted to be molecular [5–8]), the reason being that the $\bar{D}\Xi_c$ and $\bar{D}^*\Xi_c$ diagonal potentials

*mpavon@buaa.edu.cn

Published by the American Physical Society under the terms of the [Creative Commons Attribution 4.0 International license](https://creativecommons.org/licenses/by/4.0/). Further distribution of this work must maintain attribution to the author(s) and the published article's title, journal citation, and DOI. Funded by SCOAP³.

are exactly the same (with corrections originating from coupled channel effects from the mixing with nearby thresholds [6,8]). Indeed, a series of previous works have predicted the existence of a $\bar{D}\Xi_c$ bound state [9–14], with the more recent predictions of its mass relatively close to where it has been finally detected, e.g., (4316–4322) MeV in [11], (4329–4337) MeV in [12], 4311 MeV in [13], and (4319–4327) MeV in [14]. It should be stressed that this does not necessarily mean that the $P_{\psi s}^{\Lambda}(4338)$ and $P_{\psi s}^{\Lambda}(4459)$ are composite, only that they are compatible with the molecular hypothesis (see also the recent discussion in [15,16]; for nonmolecular pentaquark models check [17–20]). Yet, from a Bayesian perspective the convergence of the previous predictions (which rely on different assumptions: phenomenological [11–13] or effective [14]) reinforces the belief that they might be predominantly meson-baryon bound states or resonances.

II. EFFECTIVE FIELD THEORY DESCRIPTION

We will consider the $P_{\psi s}^{\Lambda}(4338)$ and $P_{\psi s}^{\Lambda}(4459)$ as poles in the $\bar{D}\Xi_c$ and $\bar{D}^*\Xi_c$ two-body scattering amplitude within a contact-range theory. With this choice, and if we include the $\bar{D}_s\Lambda - \bar{D}\Xi_c$ coupled channel dynamics, it will be possible to reproduce the $P_{\psi s}^{\Lambda}(4338)$ as a pole above the $\bar{D}\Xi_c$ threshold. We will briefly comment on the question of whether these poles can be interpreted as hadronic molecules at the end of this section, though we advance that we will only use this nomenclature for poles below their relevant thresholds.

We describe the two-body interaction within an effective field theory (EFT) where the low energy degrees of freedom are the charmed hadrons and the pions (when relevant). EFTs exploit the existence of a separation of scales in a particular physical system with the aim of writing scattering amplitudes and observables as a power series in terms of the ratio Q/M , where Q and M are characteristic low and high energy scales, respectively ($Q \ll M$). For hadronic molecules Q can be identified with the wave number γ of the bound state, $\gamma = \sqrt{2\mu B_E}$ with μ the reduced mass of the system and B_E its binding energy, while M represents the vector meson mass or the momentum at which we see the internal structure of the hadrons. That is, in general we expect $Q \sim (100\text{--}200)$ MeV and $M \sim (0.5\text{--}1.0)$ GeV give or take. EFT describes hadronic molecules in terms of a nonrelativistic potential composed of a finite- and contact-range piece. The finite-range piece, which is given by pion exchanges, can be safely neglected at the lowest order in the expansion (where one pion exchange is either not allowed owing to HQSS or perturbative and thus subleading [14]). The contact-range piece, the only one that survives here, represents the physics at the momentum scale M , and we write it down as

$$\langle \vec{p}' | V_C | \vec{p} \rangle = c = \sum_R \lambda_R c_R, \quad (2)$$

with \vec{p} and \vec{p}' the center-of-mass momenta of the initial and final hadron pair, and where c is a coupling that can be further subdivided in a sum over R —the possible quantum numbers or irreducible representations of the two-body system under consideration—with λ_R coefficients. This potential is singular (it corresponds to a Dirac-delta in r space) but can be easily regularized by the introduction of a cutoff Λ and regulator function,

$$\langle \vec{p}' | V_C(\Lambda) | \vec{p} \rangle = c(\Lambda) f\left(\frac{p'}{\Lambda}\right) f\left(\frac{p}{\Lambda}\right), \quad (3)$$

and renormalized by making the coupling dependent on Λ , i.e., $c = c(\Lambda)$, and then calibrating this coupling from the condition of reproducing an observable quantity (for instance, the binding energy, in which case it becomes an input of the theory instead of a prediction). Along this work we will use a Gaussian regulator, $f(x) = e^{-x^2}$, and a cutoff $\Lambda = 0.75$ GeV, i.e., of the order of the breakdown scale M of the EFT [in particular in the middle of the (0.5–1.0) GeV window we previously estimated for M]. For scattering amplitudes with a well-defined $\Lambda \rightarrow \infty$ limit,¹ the finite

¹Even if this condition is not met, from a more phenomenological perspective a cutoff of the order of the ρ meson mass is also a good choice: it maximizes the momenta at which the contact-range description is valid ($k < \Lambda$) while not being hard enough as to resolve the short-range details of the meson-baryon interaction (which happens at $\Lambda > m_\rho$ if the short-range interaction is generated by vector meson exchanges).

cutoff error Q/Λ will be similar to the EFT truncation error Q/M for $\Lambda \sim M$. We will explicitly check whether the cutoff uncertainties are under control by doubling its value, i.e., we will compare the predictions of the meson-baryon spectrum for $\Lambda = 0.75$ and 1.5 GeV.

For the calculation of the poles of the two-body scattering amplitude we use the bound state equation, which for the contact-range potential of Eq. (3) can be written as

$$1 + c(\Lambda) \int \frac{d^3 \vec{p}}{(2\pi)^3} \frac{f^2(p/\Lambda)}{M_{\text{th}} + \frac{p^2}{2\mu} - M_{\text{mol}}} = 0, \quad (4)$$

where M_{mol} is the mass of the state we are predicting, M_{th} the two-body threshold and μ the reduced mass of the two-body system. The evaluation of the loop integral takes the general form

$$\int \frac{d^3 \vec{p}}{(2\pi)^3} \frac{f^2(p/\Lambda)}{M_{\text{th}} + \frac{p^2}{2\mu} - M_{\text{mol}}} = -\frac{\mu}{2\pi} \left[\gamma + \Lambda \beta \left(\frac{\gamma}{\Lambda} \right) \right], \quad (5)$$

with $\gamma = \sqrt{2\mu(M_{\text{th}} - M_{\text{mol}})}$ the wave number of the two-body system and β a regulator dependent function. By taking $\text{Re}[\gamma] > 0$ ($\text{Re}[\gamma] < 0$) we will choose Riemann sheet I (II). Solutions in sheet I (II) correspond to bound (virtual) states. For the generalization to coupled channels we define

$$F_{ab} = \delta_{ab} + c_{ab}(\Lambda) \int \frac{d^3 \vec{p}}{(2\pi)^3} \frac{f^2(p/\Lambda)}{M_{\text{th}(b)} + \frac{p^2}{2\mu_b} - M_{\text{mol}}}, \quad (6)$$

with the indices a, b labeling the channels. The states (or poles) now correspond to

$$\det(F) = 0, \quad (7)$$

where depending on the combination of Riemann sheets (there are two sheets per channel: $\text{Re}[\gamma_a] > 0$ and $\text{Re}[\gamma_a] < 0$) we will talk of bound/virtual states or resonances.

For the complete EFT description of the $\bar{D}^{(*)}\Xi_c$ system we will refer to [6,14] for further details. Here we will present an abridged version of Ref. [14], which proposed three possible power countings— A , B , and C —for pentaquarks containing either antitriplet or sextet charmed baryons. Power counting B is restricted to the $\bar{H}_c T_c$ systems, with $H_c = D, D_s$ or D^*, D_s^* and $T_c = \Lambda_c, \Xi_c$, and hence well suited for the new Λ -like pentaquarks. Within it, the $P_{\psi_s}^\Lambda(4338/4459)$ is described as a $\bar{D}_s^{(*)}\Lambda_c - \bar{D}^{(*)}\Xi_c$ coupled channel system with the contact-range potential

$$V_C(P_{\psi_s}^\Lambda) = \begin{pmatrix} \frac{1}{2}(d_a + \tilde{d}_a) & \frac{1}{\sqrt{2}}(d_a - \tilde{d}_a) \\ \frac{1}{\sqrt{2}}(d_a - \tilde{d}_a) & d_a \end{pmatrix}, \quad (8)$$

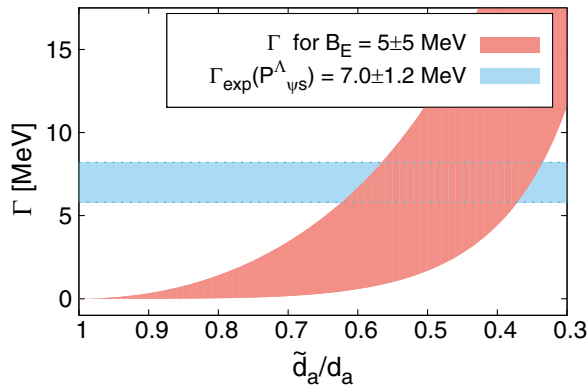


FIG. 1. Partial decay width of a shallow $\bar{D}\Xi_c$ bound state into $\bar{D}_s\Lambda_c$ as a function of the ratio of the \tilde{d}_a and d_a couplings in the contact-range EFT described by Eq. (8). The binding energy of the state is $B_E = (5 \pm 5)$ MeV and the cutoff is set to $\Lambda = 0.75$ GeV. It can be appreciated that the width grows with the ratio between \tilde{d}_a and d_a . For comparison, we show the experimental width of the $P_{\psi_s}^\Lambda(4338)$ pentaquark.

with d_a and \tilde{d}_a two independent coupling constants, while for the other $\bar{H}_c T_c$ systems we have

$$V_C(P_\psi^N/P_\psi^\Sigma/P_\psi^\Xi) = \tilde{d}_a. \quad (9)$$

The coupling d_a represents the strength of the diagonal $\bar{D}^{(*)}\Xi_c$ interaction and the $(d_a - \tilde{d}_a)/\sqrt{2}$ linear combination determines the partial decay width into the $\bar{D}_s^{(*)}\Lambda_c$ decay channel, which we illustrate in Fig. 1 for a shallow $\bar{D}\Xi$ bound state. Thus, we can determine these two couplings from the mass and width of a given Λ -like hidden charm pentaquark, which is done by solving Eqs. (6) and (7) with the $\bar{D}_s^{(*)}\Lambda_c - \bar{D}^{(*)}\Xi_c$ potential of Eq. (8) in the (II,I) Riemann sheet.

For the choice of input (i.e., Λ -like pentaquark), we will either take the newly discovered $P_{\psi_s}^\Lambda(4338)$ or the previous $P_{\psi_s}^\Lambda(4459)$. For the latter, there are a single- and a double-peak determination of its mass [4], with the single-peak mass and width being:

$$\begin{aligned} M(P_{\psi_s}^\Lambda) &= 4458.8 \pm 2.9_{-1.1}^{+4.7} \text{ MeV}, \\ \Gamma(P_{\psi_s}^\Lambda) &= 17.3 \pm 6.5_{-5.7}^{+8.0} \text{ MeV}, \end{aligned} \quad (10)$$

and the double-peak:

$$\begin{aligned} M(P_{\psi_s1}^\Lambda) &= 4454.9 \pm 2.7 \text{ MeV}, \\ \Gamma(P_{\psi_s1}^\Lambda) &= 7.5 \pm 9.7 \text{ MeV}, \end{aligned} \quad (11)$$

$$\begin{aligned} M(P_{\psi_s2}^\Lambda) &= 4467.8 \pm 3.7 \text{ MeV}, \\ \Gamma(P_{\psi_s2}^\Lambda) &= 5.3 \pm 5.3 \text{ MeV}. \end{aligned} \quad (12)$$

From HQSS we indeed expect the existence of two $J = \frac{1}{2}, \frac{3}{2}$ $\bar{D}^*\Xi_c$ bound states, as their diagonal potential is exactly the same (there is no spin dependence). This degeneracy will be broken by coupled-channel effects, which are naively expected to be small in comparison with the diagonal interaction. Reality might be more ambiguous than expectations though, with Ref. [6,14] finding that the effect of the nearby $\bar{D}\Xi_c'$ and $\bar{D}\Xi_c^*$ channels ranges between leading order (LO) and next-to-leading order in size. This means that for a LO calculation one might ignore the aforementioned coupled channel dynamics and still use either of the previous two poles as input at the price of a slower convergence rate (the relative LO uncertainty with and without the $\bar{D}\Xi_c'$ and $\bar{D}\Xi_c^*$ coupled channels is estimated to be about 0.27 and $(0.54 - 0.60)$, respectively, for the $P_{\psi_s}^\Lambda(4459)$ as a $\bar{D}^*\Xi_c$ molecule [6]). Alternatively we might average the masses and widths of the two peaks, which partially cancels out the effects of the coupled channel dynamics. What we will do then is to use either the single peak solution, each of the double peak solutions or the average of the double peak solutions, i.e.,

$$\begin{aligned} M(P_{\psi_s12}^\Lambda) &= 4461.4 \pm 2.4 \text{ MeV}, \\ \Gamma(P_{\psi_s12}^\Lambda) &= 6.4 \pm 5.5 \text{ MeV}, \end{aligned} \quad (13)$$

for the determination of d_a and \tilde{d}_a from $P_{\psi_s}^\Lambda(4459)$, giving us a total of five possible determinations.

Here a few comments are in order. The first is that the $P_{\psi_s}^\Lambda(4338)$ is close to the $\bar{D}\Xi_c$ threshold and, as a consequence, its Breit-Wigner mass and width are likely to differ from that of the pole in the scattering amplitude [21–23] (if it happens to be a composite state). Indeed, the couplings and spectrum that we will derive from $P_{\psi_s}^\Lambda(4338)$ are outliers, being different than those derived from the $P_{\psi_s}^\Lambda(4459)$.

Second, using the width as input implicitly assumes that the decay width is saturated by the meson-baryon partial width. In this regard, if we consider the $P_\psi^N(4312)$ —suspected to be a $\bar{D}\Sigma_c$ bound state [24–30]—the GlueX experiment [31] found that its branching ratio into $J/\psi N$ is of the order of the single digit percentages. That is, the $P_\psi^N(4312)$ width is mostly saturated by $\bar{D}^*\Lambda_c$ (except for a small contribution coming from the width of the Σ_c). Analogously, we will assume the widths of the $P_{\psi_s}^\Lambda(4338/4459)$ to be saturated by $\bar{D}_s\Lambda_c/\bar{D}_s^*\Lambda_c$.

Third, in its current implementation our calculations are not convergent for $\Lambda \rightarrow \infty$, which eventually manifests as a strong cutoff dependence for $\Lambda \gg M$. The reason is the existence of pairs of channels for which the potential is identical as a consequence of a symmetry but for which the reduced masses μ and μ' are not identical (e.g., $\bar{D}\Xi_c$ and $\bar{D}^*\Xi_c$ with HQSS). This eventually generates a divergence proportional to $\Delta\mu = \mu' - \mu$ for large enough cutoffs for the state that is being predicted. Basically, the physical masses

TABLE I. Predictions of the $\bar{H}_c T_c$ bound/virtual states and resonances (the masses are in units of MeV) from the $P_{\psi_s}^\Lambda(4338/4459)$, depending on the specific choice of input. The spectrum is calculated for two different cutoffs, $\Lambda = 0.75$ and 1.5 GeV, where the masses are shown in the format $M(\Lambda = 0.75 \text{ GeV}) - M(\Lambda = 1.5 \text{ GeV})$. Set B_1 uses the $P_{\psi_s}^\Lambda(4338)$ as input [i.e., as “ M_{mol} ” in Eqs. (6) and (7) with the potential of Eq. (8)], leading to the couplings $d_a = -(0.98 - 0.42) \text{ fm}^2$ and $\tilde{d}_a = -(0.26 - 0.25) \text{ fm}^2$ for $\Lambda = (0.75-1.5) \text{ GeV}$; set B_2 uses the $P_{\psi_s}^\Lambda(4459)$ single-peak solution [$d_a = -(1.59 - 0.54) \text{ fm}^2$, $\tilde{d}_a = -(0.79 - 0.39) \text{ fm}^2$]; set B_3 uses the lower mass pentaquark ($P_{\psi_{s1}}^\Lambda$, $M = 4454.9 \text{ MeV}$) of the double-peak solution for the $P_{\psi_s}^\Lambda(4459)$ ($d_a = -(1.54 - 0.54) \text{ fm}^2$, $\tilde{d}_a = -(1.02 - 0.44) \text{ fm}^2$); set B_4 uses the higher mass pentaquark ($P_{\psi_{s2}}^\Lambda$, $M = 4467.8 \text{ MeV}$) of the double-peak solution ($d_a = -(1.23 - 0.48) \text{ fm}^2$, $\tilde{d}_a = -(0.78 - 0.38) \text{ fm}^2$); finally, set B_5 uses the average of $P_{\psi_{s1}}^\Lambda$ and $P_{\psi_{s2}}^\Lambda$ as input ($d_a = -(1.39 - 0.51) \text{ fm}^2$, $\tilde{d}_a = -(0.91 - 0.41) \text{ fm}^2$). The masses of the N -, Σ -, and Ξ -like pentaquarks are determined from solving Eq. (4) with the potential of Eq. (9). The superscript V indicates a virtual state. For the $\bar{D}\Xi_c$ and $\bar{D}^*\Xi_c$ states we do not show the width, as it basically coincides with the width of the input state (within half a MeV). Calculations are done in the isospin symmetric limit by averaging the masses listed in the Review of Particle Physics [36].

System	Type	Set B_1	Set B_2	Set B_3	Set B_4	Set B_5
$\bar{D}\Lambda_c$	P_ψ^N	(4111.3 – 4120.2) ^V	(4153.7 – 4153.6) ^V	4150.9 – 4152.0	(4153.7 – 4153.5) ^V	4152.9 – 4153.4
$\bar{D}^*\Lambda_c$	P_ψ^N	(4256.7 – 4267.7) ^V	4295.0 – 4295.0	4291.4 – 4291.8	4295.0 – 4295.0	4293.7 – 4293.9
$\bar{D}_s\Lambda_c$	$P_{\psi_s}^\Lambda$	4254.8 – 4254.7	4233.9 – 4239.4	4237.1 – 4240.3	4249.5 – 4251.1	4243.7 – 4246.1
$\bar{D}_s^*\Lambda_c$	$P_{\psi_s}^\Lambda$	4398.4 – 4398.5	4375.2 – 4378.5	4378.9 – 4380.1	4392.1 – 4392.7	4385.9 – 4386.8
$\bar{D}\Xi_c$	$P_{\psi_s}^\Lambda$	Input	4319.0 – 4321.0	4315.5 – 4317.7	4327.8 – 4329.2	4321.7 – 4323.6
$\bar{D}^*\Xi_c$	$P_{\psi_s}^\Lambda$	4479.2 – 4478.7	Input	Input	Input	Input
$\bar{D}\Xi_c$	$P_{\psi_s}^\Sigma$	(4297.4 – 4308.2) ^V	4336.3 – 4336.2	4332.8 – 4333.3	4336.3 – 4336.3	4335.1 – 4335.4
$\bar{D}^*\Xi_c$	$P_{\psi_s}^\Sigma$	(4442.7 – 4455.3) ^V	4477.5 – 4477.3	4473.1 – 4472.6	4477.5 – 4477.4	4475.8 – 4475.4
$\bar{D}_s\Xi_c$	$P_{\psi_{ss}}^\Xi$	(4401.4 – 4413.5) ^V	4437.3 – 4437.2	4433.2 – 4433.0	4437.3 – 4437.3	4435.7 – 4435.6
$\bar{D}_s^*\Xi_c$	$P_{\psi_{ss}}^\Xi$	(4548.3 – 4562.3) ^V	4580.9 – 4580.4	4576.1 – 4574.7	4581.0 – 4580.6	4579.0 – 4578.0

are breaking a symmetry of the potential (e.g., the difference in the reduced masses between $\bar{D}\Xi_c$ and $\bar{D}^*\Xi_c$, which violates HQSS) and this manifests as a divergence. Calculations can be rendered cutoff independent by including $\Delta\mu$ as a subleading correction.^{2,3} Yet, predictions from calculations with the physical masses, which are formally divergent, turn out to have a weak to moderate cutoff dependence for $\Lambda \sim M$, see Refs. [26,28,34,35] for a few examples involving molecular pentaquarks and cutoffs ranging from 0.5 to 1.5 GeV. For this reason we follow this later choice (i.e., we use the physical masses), even though *stricto sensu* it is not a genuine EFT calculation but rather an EFT-inspired calculation.

Fourth, there is the issue of whether the $P_{\psi_s}^\Lambda(4338)$ can be considered molecular or not: its relative center-of-mass energy with respect to the $\bar{D}\Xi_c$ threshold is $(1.9 - 3.5i) \text{ MeV}$ (in the isospin symmetric limit), where its imaginary part is larger than the real one. In the semiclassical picture this can be interpreted as the $\bar{D}\Xi_c$ pair

²In this case it will be possible to take the $\Lambda \rightarrow \infty$ limit and end up with an EFT without a cutoff [e.g., the description of the $X(3872)$ as a \bar{D}^*D molecule found in [32]].

³This solution only works for symmetries connecting both the potentials and the masses of the particles. If the masses are not related by symmetry (but the potentials are), as happens with heavy flavor symmetry, it is impossible to reformulate the theory in a cutoff independent way, as demonstrated in [33].

dissociating before they orbit each other even once, which does not comply with our intuitive understanding of a molecule. For this reason we will not use the term molecular when referring to the $P_{\psi_s}^\Lambda(4338)$ and reserve it to relatively narrow states below a nearby two-body threshold.

III. PREDICTIONS

For each of the five determinations considered we predict the spectrum shown in Table I: set B_1 within the table indicates the predictions derived from the $P_{\psi_s}^\Lambda(4338)$, while sets B_2, B_3, B_4, B_5 instead use the $P_{\psi_s}^\Lambda(4459)$ (as previously explained) as input. It is worth commenting that predictions from set B_1 are relatively different from the other sets, which comes as a consequence of the mass and width of the $P_{\psi_s}^\Lambda(4338)$ (in particular that it is located above the $\bar{D}\Xi_c$ threshold). If the $P_{\psi_s}^\Lambda(4338)$ turns out to be below this threshold or is more narrow than its Breit-Wigner determination, it will imply a larger \tilde{d}_a/d_a ratio (as in Fig. 1) and thus predictions more in line to those of sets B_2, B_3, B_4 , and B_5 . We also notice that the input dependence of the predictions (the differences among the aforementioned sets) is larger than their cutoff dependence within the $\Lambda = (0.75-1.5) \text{ GeV}$ range. In Table I it can also be appreciated that the farther a state is predicted from threshold the larger its cutoff dependence is.

The first and most robust prediction is that of the $\bar{D}_s^{(*)}\Lambda_c$ pentaquarks, which bind for all of the sets considered (though, depending on the input, predictions vary within a mass range of 20 MeV and are thus still compatible with these two systems not binding). The $\bar{D}_s\Lambda_c$ ($\bar{D}_s^*\Lambda_c$) partner of the $P_{\psi s}^\Lambda(4338)$ [$P_{\psi s}^\Lambda(4459)$] is located at (4235–4255) MeV [(4375–4390) MeV]. If bound, these pentaquark are expected to be relatively narrow, as their decay into an anticharmed meson-charmed baryon pair is forbidden.

A second interesting prediction is that of an isovector $\bar{D}\Xi_c$ molecule with a mass in the 4335 MeV region, i.e., a $P_{\psi s}^\Sigma(4335)$ pentaquark. However this state is only there when we use the $P_{\psi s}^\Lambda(4459)$ pentaquark as the input for the determination of the parameters (but not if the $P_{\psi s}^\Lambda(4338)$ is used). From this, it is apparent that the prediction of the $P_{\psi s}^\Sigma(4335)$ is more tentative in nature than that of the $\bar{D}_s^{(*)}\Lambda_c$ bound states. This $P_{\psi s}^\Sigma$ has been previously predicted in [14] (EFT) or more recently in [37] (QCD sum rules). If molecular, it should be relative narrow. Its neutral component $P_{\psi s}^{\Sigma^0}$ will have a small $J/\psi\Lambda$ decay width owing to isospin breaking effects, which are easy to quantify. From SU(3)-flavor symmetry we expect the $\bar{D}\Xi_c(I=0, 1)$ decay amplitude into $J/\psi\Lambda$ and $J/\psi\Sigma$ to be related as follows

$$\langle \bar{D}\Xi_c(I=0) | H | J/\psi\Lambda \rangle = -\frac{1}{\sqrt{3}} \langle \bar{D}\Xi_c(I=1) | H | J/\psi\Sigma \rangle, \quad (14)$$

from which it is easy to work out that the isospin breaking branching ratio of a molecular $P_{\psi s}^{\Sigma^0}$ into these two decay channels will be

$$\frac{\Gamma(P_{\psi s}^{\Sigma^0} \rightarrow J/\psi\Lambda)}{\Gamma(P_{\psi s}^{\Sigma^0} \rightarrow J/\psi\Sigma^0)} = \frac{1}{3} \frac{p_\Lambda}{p_\Sigma} \left| \frac{\Psi_c(0) - \Psi_n(0)}{\Psi_c(0) + \Psi_n(0)} \right|^2, \quad (15)$$

where $p_{\Lambda/\Sigma}$ refers to the center-of-mass momentum of the final charmonium-baryon pair, while $\Psi_c(r)$ and $\Psi_n(r)$ are the charged ($D^-\Xi_c^+$) and neutral ($\bar{D}^0\Xi_c^0$) components of the $P_{\psi s}^{\Sigma^0}$ r -space wave function evaluated at the origin ($r=0$). For the four determinations of the couplings where there is a $P_{\psi s}^\Sigma$ close to threshold, we obtain a branching ratio of $(0.7 - 2.4) \times 10^{-2}$, $(0.2 - 0.4) \times 10^{-2}$, $(3.1 - 6.4) \times 10^{-2}$ and $(0.6 - 1.6) \times 10^{-2}$ for sets B_2 , B_3 , B_4 , and B_5 , respectively, and cutoff $\Lambda = (0.75-1.5)$ GeV, where the closer the prediction to threshold (B_2 and B_4 , see Table I) the larger the branching.

From the previous in a first approximation this isovector $\bar{D}\Xi_c$ state is not likely to be easily detectable in the $J/\psi\Lambda$ invariant mass. Yet, caution is advised. A closer look at the isospin breaking potential, i.e.,

$$V_C(\bar{D}^0\Xi_c^0 - D^-\Xi_c^+) = \begin{pmatrix} \frac{1}{2}(d_a + \tilde{d}_a) & -\frac{1}{2}(d_a - \tilde{d}_a) \\ -\frac{1}{2}(d_a - \tilde{d}_a) & \frac{1}{2}(d_a + \tilde{d}_a) \end{pmatrix}, \quad (16)$$

reveals an interesting pattern: the $(d_a - \tilde{d}_a)$ linear combination does not only control the meson-baryon decay width of the $P_{\psi s}^\Lambda$ but also the size of isospin breaking in $P_{\psi s}^{\Sigma^0}$. For $d_a = \tilde{d}_a$ we will have twin $\bar{D}^0\Xi_c^0$ and $D^-\Xi_c^+$ bound states with the same binding energy and an isospin breaking branching ratio of $p_\Lambda/(3p_\Sigma) \simeq 0.5$, see Eq. (15). This is well above the $\mathcal{O}(10^{-2})$ values we obtained for sets B_2 to B_5 . If $|d_a| > |\tilde{d}_a|$ the higher mass $D^-\Xi_c^+$ state will become the isovector $P_{\psi s}^{\Sigma^0}$ pentaquark and, as the difference between the two couplings increases, the branching ratio will decrease. That is, if the mass splitting between the $P_{\psi s}^\Lambda$ and $P_{\psi s}^{\Sigma^0}$ is not considerably larger than the mass difference between the $\bar{D}^0\Xi_c^0$ and $D^-\Xi_c^+$ thresholds (2.1 MeV), the branching ratio might be sizable. If this were to be the case, the observed $P_{\psi s}^\Lambda(4338)$ peak might actually be a mixture of a $P_{\psi s}^\Lambda$ and $P_{\psi s}^{\Sigma^0}$ state.

The third prediction that is worth noticing is that of $\bar{D}^{(*)}\Lambda_c$ bound states, which are again only found when using the $P_{\psi s}^\Lambda(4459)$ as input. In particular, we find a $\bar{D}\Lambda_c$ bound state at about 4150 MeV—a $P_\psi^N(4150)$ pentaquark—that might correspond with a possible structure in the $J/\psi p$ invariant mass mentioned in [1,2] (though its mass is only reported in [1]). There, when the amplitude contribution from a P_ψ^N pentaquark is included, the parameters of this pentaquark happen to be

$$M(P_\psi^N) = 4152.3 \pm 2.0 \text{ MeV}, \\ \Gamma(P_\psi^N) = 41.8 \pm 6.0 \text{ MeV}, \quad (17)$$

while the mass and width of the $P_{\psi s}^\Lambda$ are left almost unchanged [1]. Yet, there is a moderate statistical preference for the amplitude model in which this Breit-Wigner contribution is not present. Were there to be a $\bar{D}\Lambda_c$ virtual or bound state close to threshold, the Breit-Wigner parametrization is unlikely to be an ideal choice. It is also worth noticing that within the one-boson-exchange model the $\bar{D}^{(*)}\Lambda_c$ and $\bar{D}^{(*)}\Lambda_c(2595/2625)$ potentials only involve the σ and ω mesons, probably with similar couplings and cutoffs, i.e., if one of these systems binds the other is also likely to bind. In this regard there are previous phenomenological predictions of $\bar{D}\Lambda_c$ [38,39] and $\bar{D}\Lambda_c(2595)$ [40] bound states and arguments for the interpretation of the $P_\psi^N(4457)$ as a $\bar{D}\Lambda_c(2595)$ state [41] [instead of the more usual $\bar{D}^*\Sigma_c$ identification, which has been argued not to fully explain the $P_\psi^N(4457)$ [42,43]]. However, the existence of an unusually long-ranged, $L=1$ one pion exchange force in the $\bar{D}\Lambda_c(2595)$ system [44,45] has also

been shown to make binding much more easy in this case [46]. As a consequence, the eventual confirmation of a $\bar{D}\Lambda_c(2595)$ bound state might merely signal the existence of moderate attraction in $\bar{D}\Lambda_c$, but not necessarily binding.

IV. FURTHER CONSIDERATIONS REGARDING THE $P_{\psi s}^\Lambda(4255)$

More information might be extracted about the $P_{\psi s}^\Lambda(4338)$ and its conjectured lower mass partner from two recent analyses of the invariant mass distributions in [47,48].

The amplitude analysis of the $J/\psi\Lambda$ spectrum of Burns and Swanson [47] suggests that there is no $P_{\psi s}^\Lambda(4338)$ in the first place, but a triangle singularity instead. It is important to notice that their analysis includes the assumption that $\tilde{d}_a \geq 0$ though.⁴ This is incompatible with the determinations we obtain here, which consistently gets $\tilde{d}_a < 0$. Had we imposed the condition $\tilde{d}_a \geq 0$, it would have simply been impossible to reproduce the $P_{\psi s}^\Lambda(4338)$ as a resonance in the (II,I) Riemann sheet. However, with this constraint we are still able to generate a pole with the experimental mass of the $P_{\psi s}^\Lambda(4338)$ in the (I,II) Riemann sheet—that is, a sheet that does not influence physical $\bar{D}\Xi_c$ scattering—for $d_a = -(0.62 - 0.25) \text{ fm}^2$ ($\Lambda = (0.75-1.5) \text{ GeV}$) and $\tilde{d}_a = 0$. This coupling also implies the existence of a $\bar{D}_s\Lambda_c$ virtual state with mass $M = (4219.9 - 4167.3)^V \text{ MeV}$, which is not expected to be observable either (it is far from threshold and in the second Riemann sheet). That is, if we impose the same assumptions as in [47] we also reach the conclusion that the $P_{\psi s}^\Lambda(4338)$ is not a $\bar{D}\Xi_c$ scattering pole.

In contrast, the amplitude analysis of Nakamura and Wu [48] explains the $P_{\psi s}^\Lambda(4338)$ as a $\bar{D}\Xi_c$ state and predicts the existence of a virtual $\bar{D}_s\Lambda_c$ pole. In their analysis the mass and width of the $P_{\psi s}^\Lambda(4338)$ are [48]

$$M = 4338.0 \pm 1.1 \text{ MeV}, \quad (18)$$

$$\Gamma = 1.7 \pm 0.4 \text{ MeV}, \quad (19)$$

which is narrower than its usual determination from a Breit-Wigner profile. From the previous mass and width we

⁴This condition commonly appears in models that saturate \tilde{d}_a from vector meson exchange [10]. Yet, this does not take into account the existence of unaccounted attraction from other sources (e.g., two-pion exchange). For comparison, had we applied this criterion to the neutron-proton system, the result would have been repulsion in the S wave $S = 0, 1$ spin configurations (owing to the strongly repulsive nature of ω exchange in this system [49]), in contradiction with experimental evidence. We notice that in [47] a different linear combinations of couplings is used: $A = \tilde{d}_a$ and $\Delta = (d_a - \tilde{d}_a)/2$.

obtain the couplings $d_a = -(0.85 - 0.40) \text{ fm}^2$ and $\tilde{d}_a = -(0.25 - 0.25) \text{ fm}^2$ [for $\Lambda = (0.75-1.5) \text{ GeV}$], which at first sight are very similar to the ones obtained from the Breit-Wigner profile [namely $d_a = -(0.98 - 0.42) \text{ fm}^2$ and $\tilde{d}_a = -(0.26 - 0.25) \text{ fm}^2$, check the caption in Table I]. There is a difference though when predicting the $\bar{D}_s\Lambda_c$ pole, which is now a virtual state just below threshold:

$$M = (4253.9 - 4253.4)^V \text{ MeV}, \quad (20)$$

which is compatible with the mass extracted in [48], $M = (4254.6 \pm 0.5)^V \text{ MeV}$. The results are not expected to be identical, as the contact-range potential in [48] does not follow the constraints of SU(3)-flavor symmetry for the nondiagonal terms in Eq. (8). The possibility that the lower mass partner of the $P_{\psi s}^\Lambda(4338)$ is a virtual state is also satisfying from the point of view of the experimental information available in [2], where the conjectured $P_{\psi s}^\Lambda(4255)$ is not observed.

V. CONCLUSIONS

The $P_{\psi s}^\Lambda(4338)$ is a very interesting pentaquark, which we interpret here as a pole in the $\bar{D}\Xi_c$ scattering amplitude within a theory where the meson-baryon interaction is of a contact-range nature. On the one hand, its existence is to be expected from the $P_{\psi s}^\Lambda(4459)$: the $\bar{D}\Xi_c$ and $\bar{D}^*\Xi_c$ S -wave interactions are identical as a consequence of HQSS, except for perturbations coming from coupled channel dynamics with nearby thresholds. Thus, in a first approximation there will be $J = \frac{1}{2} \bar{D}\Xi_c$ and $J = \frac{1}{2}, \frac{3}{2} \bar{D}^*\Xi_c$ states with similar binding energies. On the other, the $\bar{D}_s^{(*)}\Lambda_c - \bar{D}_s^{(*)}\Xi_c$ coupled channel dynamics constrains not only the mass but also the width of the $P_{\psi s}^\Lambda(4338/4459)$ pentaquarks. This observation allows us to infer more information about the interaction of the pentaquarks containing an antitriplet charmed baryon and an anticharmed meson and predict new states. The most probable of these predictions is the existence of lower mass, $\bar{D}_s^{(*)}\Lambda_c$ partners of the $P_{\psi s}^\Lambda(4338/4459)$, which we denote $P_{\psi s}^\Lambda(4250)$ and $P_{\psi s}^\Lambda(4385)$ in reference to their masses. Next, though less probable, there might be hints of the existence of an isovector partner of the $P_{\psi s}^\Lambda(4338)$ with a very similar mass—a $P_{\psi s}^\Sigma(4335)$ —also a $\bar{D}\Lambda_c$ pole close to threshold—a $P_\psi^N(4150)$ —and even $\bar{D}_s^{(*)}\Xi_c$ states, i.e., a $P_{\psi ss}^\Xi(4435)$ and $P_{\psi ss}^\Xi(4580)$.

Finally, it is worth mentioning that the description of pentaquarks as meson-baryon systems interacting via contact-range interactions indeed reproduces the masses of both the $P_{\psi s}^\Lambda(4338)$ and $P_{\psi s}^\Lambda(4459)$ as well as most other pentaquarks, with the exceptions of the $P_\psi^N(4337)$ [50] (see, e.g., [14,51]) and the broad

$P_{\psi}^N(4380)$ [52] (which we in principle distinguish from the narrow $P_{\psi}^N(4380)$ predicted in [26–30]). This does not necessarily imply that they are meson-baryon states: for this, a detailed comparison with other competing models will be necessary. Besides, the methods we use are crude and intended mostly as a proof of concept: the most important limitation is the fact that we are using the Breit-Wigner masses and widths as inputs, which do not necessarily correspond to those of the poles of the scattering amplitudes, as illustrated by a recent analysis of the $J/\psi\Lambda$ invariant mass distribution for the $P_{\psi s}^{\Lambda}(4338)$ [48] (though the competing analysis of [47] suggests that this pentaquark might be a triangle singularity). The eventual extension of this type of analyses to

the $P_{\psi s}^{\Lambda}(4459)$ might potentially confirm or refute its connection with the $P_{\psi s}^{\Lambda}(4338)$.

ACKNOWLEDGMENTS

This work is partly supported by the National Natural Science Foundation of China under Grants No. 11735003, No. 11835015, No. 11975041, No. 12047503, and No. 12125507, the Chinese Academy of Sciences under Grant No. XDB34030000, the China Postdoctoral Science Foundation under Grant No. 2022M713229, and the Fundamental Research Funds for the Central Universities and the Thousand Talents Plan for Young Professionals. M. P. V. would also like to thank the IJCLab of Orsay, where part of this work has been done, for its long-term hospitality.

-
- [1] C. Chen and E. Sparado Norella, Particle zoo 2.0: New tetra- and pentaquarks at LHCb, <https://indico.cern.ch/event/1176505/> (2022), presented at the LHC Seminar.
- [2] LHCb Collaboration, arXiv:2210.10346.
- [3] T. Gershon (LHCb Collaboration), arXiv:2206.15233.
- [4] R. Aaij *et al.* (LHCb Collaboration), *Sci. Bull.* **66**, 1278 (2021).
- [5] H.-X. Chen, W. Chen, X. Liu, and X.-H. Liu, *Eur. Phys. J. C* **81**, 409 (2021).
- [6] F.-Z. Peng, M.-J. Yan, M. Sánchez Sánchez, and M. P. Valderrama, *Eur. Phys. J. C* **81**, 666 (2021).
- [7] M.-Z. Liu, Y.-W. Pan, and L.-S. Geng, *Phys. Rev. D* **103**, 034003 (2021).
- [8] R. Chen, *Phys. Rev. D* **103**, 054007 (2021).
- [9] J.-J. Wu, R. Molina, E. Oset, and B. S. Zou, *Phys. Rev. Lett.* **105**, 232001 (2010).
- [10] C. W. Xiao, J. Nieves, and E. Oset, *Phys. Lett. B* **799**, 135051 (2019).
- [11] B. Wang, L. Meng, and S.-L. Zhu, *Phys. Rev. D* **101**, 034018 (2020).
- [12] X.-K. Dong, F.-K. Guo, and B.-S. Zou, *Prog. Phys.* **41**, 65 (2021).
- [13] C. W. Xiao, J. J. Wu, and B. S. Zou, *Phys. Rev. D* **103**, 054016 (2021).
- [14] M.-J. Yan, F.-Z. Peng, M. Sánchez Sánchez, and M. Pavon Valderrama, *Eur. Phys. J. C* **82**, 574 (2022).
- [15] M. Karliner and J. R. Rosner, *Phys. Rev. D* **106**, 036024 (2022).
- [16] F.-L. Wang and X. Liu, *Phys. Lett. B* **835**, 137583 (2022).
- [17] M. I. Eides, V. Y. Petrov, and M. V. Polyakov, *Mod. Phys. Lett. A* **35**, 2050151 (2020).
- [18] F. Stancu, *Phys. Rev. D* **101**, 094007 (2020).
- [19] J. Ferretti and E. Santopinto, *J. High Energy Phys.* **04** (2020) 119.
- [20] J. Ferretti and E. Santopinto, *Sci. Bull.* **67**, 1209 (2022).
- [21] M. Albaladejo, F.-K. Guo, C. Hidalgo-Duque, and J. Nieves, *Phys. Lett. B* **755**, 337 (2016).
- [22] C. Fernández-Ramírez, A. Pilloni, M. Albaladejo, A. Jackura, V. Mathieu, M. Mikhasenko, J. A. Silva-Castro, and A. P. Szczepaniak (JPAC Collaboration), *Phys. Rev. Lett.* **123**, 092001 (2019).
- [23] Z. Yang, X. Cao, F.-K. Guo, J. Nieves, and M. P. Valderrama, *Phys. Rev. D* **103**, 074029 (2021).
- [24] R. Chen, Z.-F. Sun, X. Liu, and S.-L. Zhu, *Phys. Rev. D* **100**, 011502 (2019).
- [25] H.-X. Chen, W. Chen, and S.-L. Zhu, *Phys. Rev. D* **100**, 051501 (2019).
- [26] M.-Z. Liu, Y.-W. Pan, F.-Z. Peng, M. Sánchez Sánchez, L.-S. Geng, A. Hosaka, and M. Pavon Valderrama, *Phys. Rev. Lett.* **122**, 242001 (2019).
- [27] C. Xiao, J. Nieves, and E. Oset, *Phys. Rev. D* **100**, 014021 (2019).
- [28] M. Pavon Valderrama, *Phys. Rev. D* **100**, 094028 (2019).
- [29] M.-Z. Liu, T.-W. Wu, M. Sánchez Sánchez, M. P. Valderrama, L.-S. Geng, and J.-J. Xie, *Phys. Rev. D* **103**, 054004 (2021).
- [30] F.-K. Guo, H.-J. Jing, U.-G. Meißner, and S. Sakai, *Phys. Rev. D* **99**, 091501 (2019).
- [31] A. Ali *et al.* (GlueX Collaboration), *Phys. Rev. Lett.* **123**, 072001 (2019).
- [32] E. Braaten and M. Kusunoki, *Phys. Rev. D* **69**, 074005 (2004).
- [33] V. Baru, E. Epelbaum, J. Gegelia, C. Hanhart, U. G. Meißner, and A. V. Nefediev, *Eur. Phys. J. C* **79**, 46 (2019).
- [34] M.-L. Du, V. Baru, F.-K. Guo, C. Hanhart, U.-G. Meißner, J. A. Oller, and Q. Wang, *Phys. Rev. Lett.* **124**, 072001 (2020).
- [35] M.-L. Du, V. Baru, F.-K. Guo, C. Hanhart, U.-G. Meißner, J. A. Oller, and Q. Wang, *J. High Energy Phys.* **08** (2021) 157.
- [36] R. L. Workman (Particle Data Group), *Prog. Theor. Exp. Phys.* **2022**, 083C01 (2022).
- [37] X.-W. Wang and Z.-G. Wang, *Chin. Phys. C* **47**, 013109 (2023).

- [38] R. Chen, A. Hosaka, and X. Liu, *Phys. Rev. D* **96**, 116012 (2017).
- [39] C.-W. Shen, D. Rönchen, U.-G. Meißner, and B.-S. Zou, *Chin. Phys. C* **42**, 023106 (2018).
- [40] T. J. Burns and E. S. Swanson, *Phys. Rev. D* **100**, 114033 (2019).
- [41] T. J. Burns and E. S. Swanson, *Phys. Rev. D* **106**, 054029 (2022).
- [42] S.-Q. Kuang, L.-Y. Dai, X.-W. Kang, and D.-L. Yao, *Eur. Phys. J. C* **80**, 433 (2020).
- [43] T. J. Burns and E. S. Swanson, *Eur. Phys. J. A* **58**, 68 (2022).
- [44] T. J. Burns, *Eur. Phys. J. A* **51**, 152 (2015).
- [45] L. Geng, J. Lu, and M. P. Valderrama, *Phys. Rev. D* **97**, 094036 (2018).
- [46] F.-Z. Peng, J.-X. Lu, M. Sánchez Sánchez, M.-J. Yan, and M. Pavon Valderrama, *Phys. Rev. D* **103**, 014023 (2021).
- [47] T. J. Burns and E. S. Swanson, *Phys. Lett. B* **838**, 137715 (2023).
- [48] S. X. Nakamura and J. J. Wu, [arXiv:2208.11995](https://arxiv.org/abs/2208.11995).
- [49] R. Machleidt, K. Holinde, and C. Elster, *Phys. Rep.* **149**, 1 (1987).
- [50] R. Aaij *et al.* (LHCb Collaboration), *Phys. Rev. Lett.* **128**, 062001 (2022).
- [51] S. X. Nakamura, A. Hosaka, and Y. Yamaguchi, *Phys. Rev. D* **104**, L091503 (2021).
- [52] R. Aaij *et al.* (LHCb Collaboration), *Phys. Rev. Lett.* **115**, 072001 (2015).